Supporting Information for

Efficient electrocatalytic glucose oxidation coupled water electrolysis driven by the Ni-foam supported Ni-P nanowire arrays

Hengwei Lou[a], Yikai Yang[b], Xiuming Bu[b], Haoxin Fan[a], Duo Weng[c], Jian Zhang[a], Wei Gao[a,d,*], Dan Wen[a,*]

[a] State Key Laboratory of Solidification Processing, School of Materials Science and Engineering, Northwestern Polytechnical University, Xi'an, 710072, P. R. China

[b] CAS Key Laboratory of Materials for Energy Conversion, Shanghai Institute of Ceramics, Chinese Academy of Sciences, Shanghai, 200050, P. R. China

[c] Shaanxi Coal Chemical Industry Technology Research Institute Co. Ltd., Xi'an, 710100, P. R. China

[d] Research & Development Institute of Northwestern Polytechnical University in Shenzhen, Shenzhen, 518057, P. R. China

[*] Corresponding authors should be addressed to W. Gao (wei.gao@nwpu.edu.cn) and D. Wen (dan.wen@nwpu.edu.cn)

1. Experimental Sections

1.1 Chemicals and materials

Sodium chloride (NaCl), sodium hypophosphite monohydrate ($NaH_2PO_2·H_2O$), hydrochloric acid (HCl), anhydrous ethanol (C_2H_6O) and concentrated sulfuric acid (H_2SO_4) were purchased from Sinopharm Chemical Reagent Co., LTD. Potassium hydroxide (KOH), anhydrous formic acid (CH_2O_2) and glucose ($C_6H_{12}O_6$) are purchased from Shanghai Aladdin biochemical Technology Co., LTD. All chemicals are used directly without further purification.

1.2 Synthesis of Ni-P@NF

Ni foam (NF) with size of 1 × 2 cm^2 was treated in anhydrous ethanol, 10 % hydrochloric acid solution, and deionized water by ultrasonication. Then, Ni foam was placed in a conical flask containing 60 mL of 0.01 M NaCl solution at 35 °C and stirred continuously for 12 h to form $Ni(OH)_2$ layer. After reaction, the obtained $Ni(OH)_2$@NF was dried in the vacuum oven at 60 °C for 1 hour. Ni-P@NF was then prepared by phosphating $Ni(OH)_2$@NF in flowing Ar atmosphere. In specific, $Ni(OH)_2$@NF was placed in the porcelain boat and 400 mg of $NaH_2PO_2·H_2O$ was located at the upstream in the tube furnace. The furnace was heated to 300 °C for 2 hours in the Ar atmosphere with a heating rate of 3 °C min^{-1}, and then naturally cooled to room temperature. To investigate the effect of phosphating temperature on the electrocatalytic performance, Ni-P@NF samples were synthesized at 300, 400, and 500 °C, respectively, for further study.

1.3 Material Characterization

The morphology and structure of the samples were characterized by transmission electron microscope (TEM, FEI Talos F200x, USA) and scanning electron microscope (SEM, FEI Nano SEM 450), and the energy-dispersive X-ray spectra (EDS) were simultaneously analyzed on Super X spectrometer. The crystalline structure of samples was studied using X-ray diffractor (XRD, Shimadzu XRD6000, Cu Kα radiation). The element composition and chemical states of the samples were analyzed by X-ray photoelectron spectroscope (XPS, Thermo Scientific ESCALAB 250Xi, USA). Raman spectra were collected using an InVia reflex confocal microscope (Renishaw, UK)

excited by a 532 nm He-Ne laser. In situ Raman measurement was also performed on the InVia reflex confocal microscope with Ni-P@NF as the working electrode, platinum wire as the counter electrode, and Ag/AgCl electrode as the reference electrodes, respectively. Each desired potential was maintained for 200 seconds to reach a steady-state condition before recording the spectrum.

1.4 Electrochemical measurements

All electrochemical tests were conducted using a three-electrode system on the CHI 660E electrochemical workstation, where HER and OER were measured in the 1 M KOH solution, and GOR was tested in the 1 M KOH solution containing 0.2 M glucose. The samples were used as the working electrodes, with graphite rod and Hg/HgO electrode functioned as the counter electrode and reference electrode, respectively. The Hg/HgO electrode was calibrated against the reversible hydrogen electrode (RHE), where $E_{RHE} = E_{Hg/HgO}+0.0591\times pH + 0.098$. The electrocatalytic activity of the samples was investigated using linear sweep voltammetry (LSV) at the scan rate of 5 mV s^{-1}. The polarization curves for GOR and OER were not iR-corrected, while it for HER was corrected with 95 % iR compensation. The electrochemical impedance spectra (EIS) were measured from 5 kHz to 0.5 Hz at -0.4 V (vs. RHE) for HER and at 1.42 V (vs. RHE) for GOR. The electrochemically active surface area (ECSA) of the samples was estimated from the electrochemical double-layer capacitance (C_{dl}) by testing the cyclic voltammetry (CV) curves with different scan rates (20, 40, 60, 80, and 100 mV s^{-1}). The stability tests of GOR, HER, overall water splitting, and the GOR-coupled water electrolysis for the Ni-P@NF sample were performed in an H-type electrolyzer using the chronoamperometry method. An anion exchange membrane (Fumasep FAA-3-50, Germany) was used to separate the cathode solution of 1 M KOH solution and the anode solution of 1 M KOH with 0.2 M glucose.

1.5 Product analysis

The oxidation products of glucose were monitored during the electrolytic process using high-performance liquid chromatography (HPLC, ECLASSICAL T3200). Before testing, the electrolyte containing glucose oxidation products was neutralized with 0.05 M H_2SO_4 solution to pH <7. The 0.01 M H_2SO_4 solution was used as the mobile phase,

with a flow rate of 0.9 mL min^{-1}. 10 μL of the electrolyte was directly injected into the Shodex SUGAR SH1011 column at 40 ℃, and the products were identified by comparing the retention time in the chromatogram with corresponding standard ones. The yield of the oxidation product was obtained according to the following equation:

$$\text{Yield (\%)} = \frac{mole\ of\ oxidation\ product}{mole\ of\ initial\ glucose} \times 100$$

The Faraday efficiency (FE) was calculated using the following equation:

$$\text{Faraday efficiency (\%)} = \frac{mole\ of\ oxidation\ product\ \times n \times F}{total\ passed\ charge} \times 100$$

where n represents the number of electrons transferred, and F is the Faraday constant.

2. Supporting figures

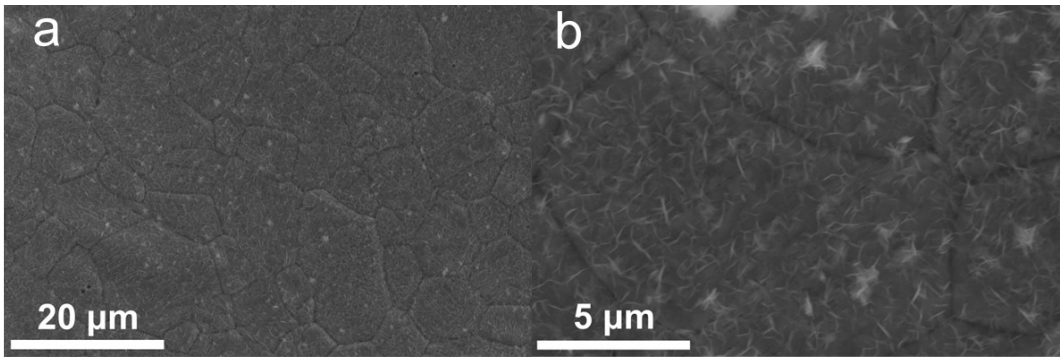

Figure S1. (a, b) SEM images of $Ni(OH)_2$@NF obtained by corrosion engineering.

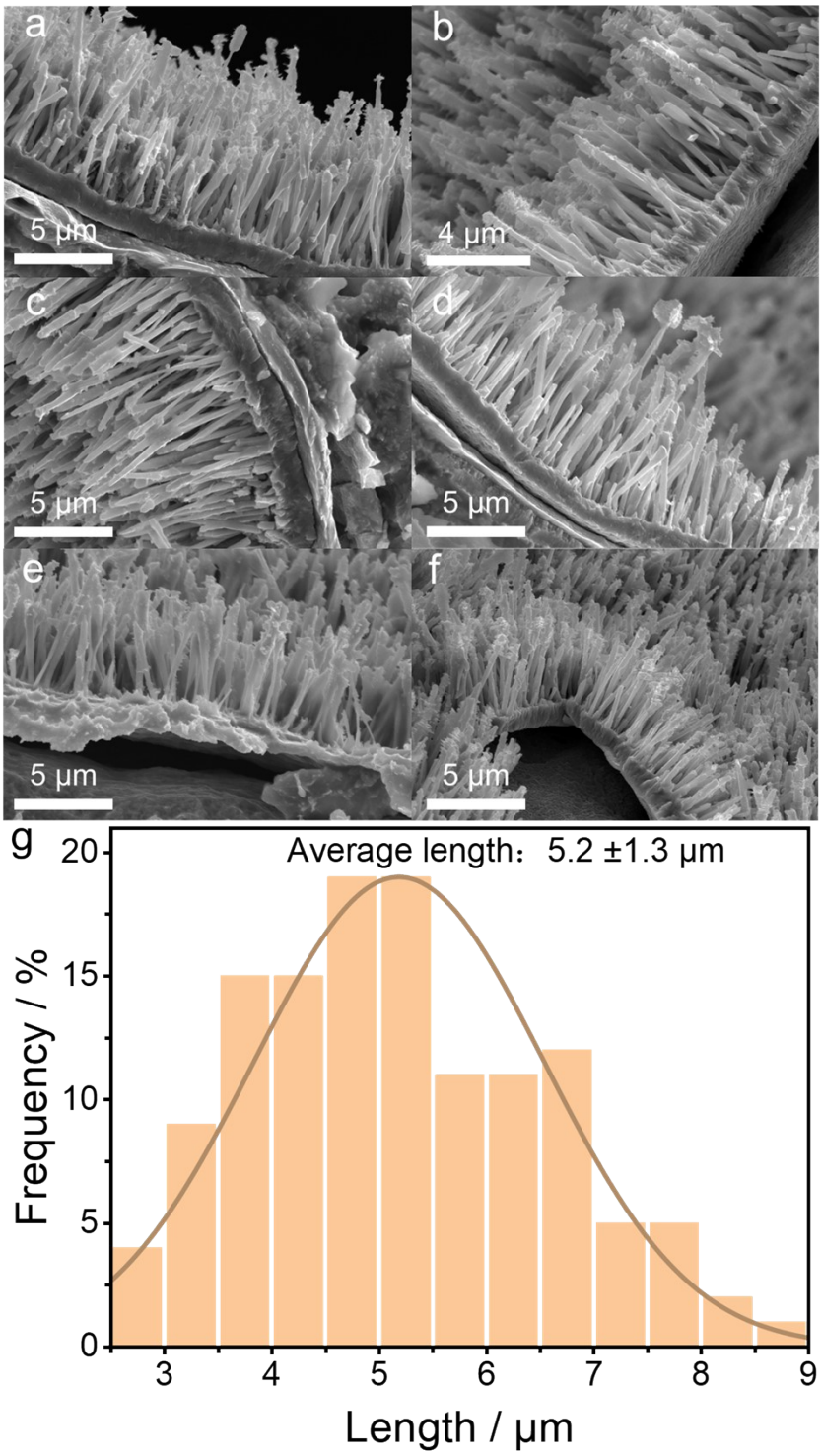

Figure S2. (a-f) SEM images of Ni-P@NF (g) Average length of Ni-P nanowires.

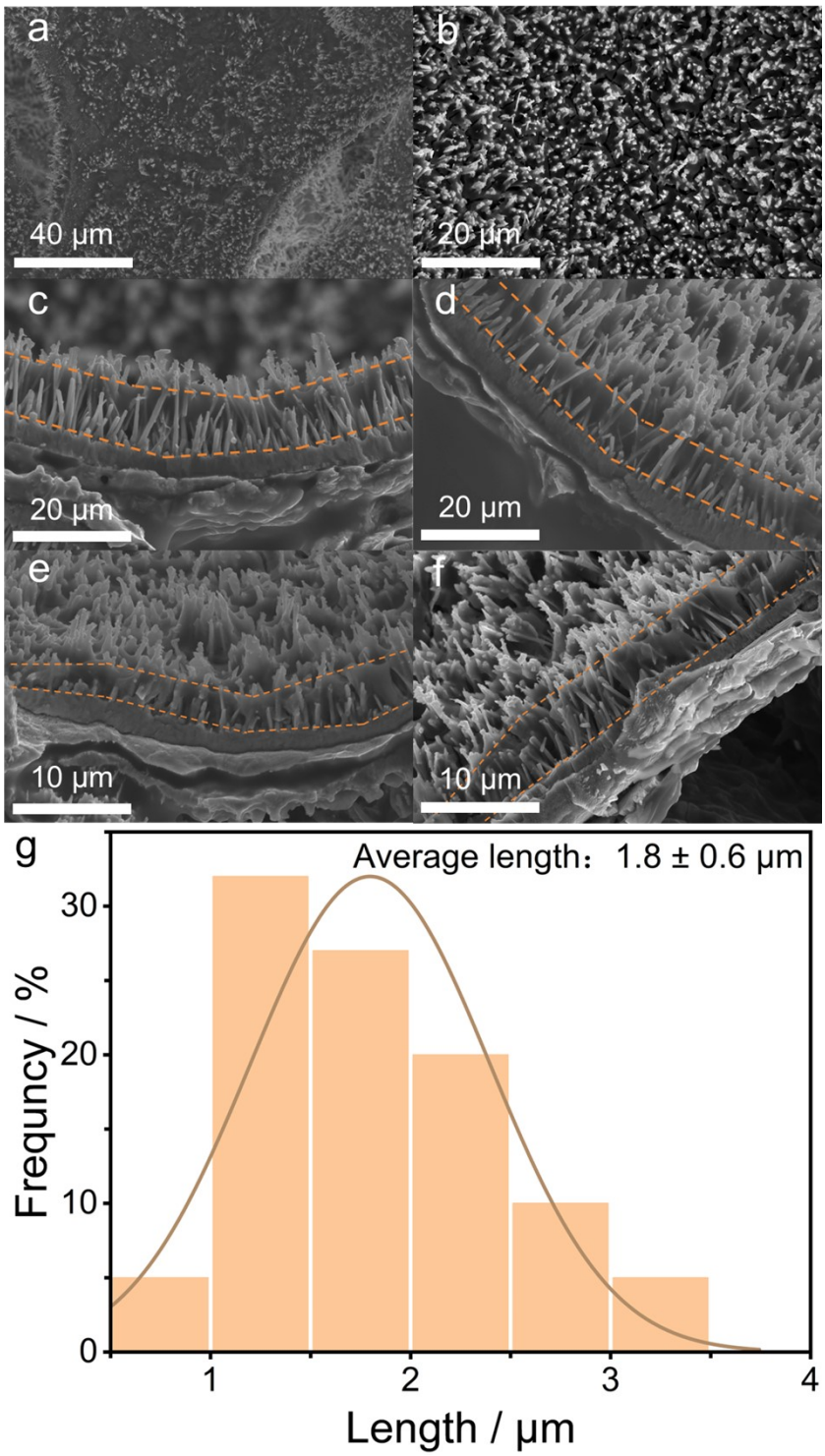

Figure S3. (a-f) SEM images of Ni-P@NF-2. (g) Average length of Ni-P nanowires.

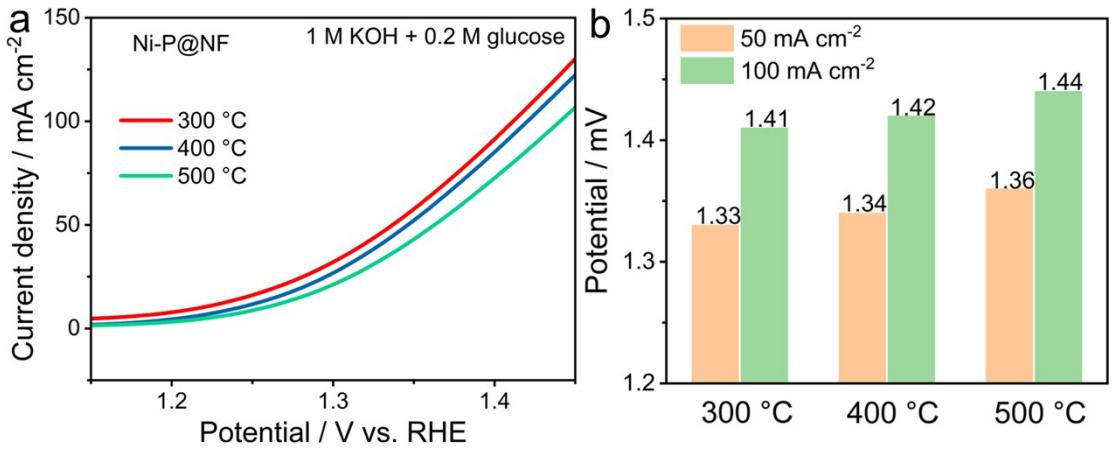

Figure S4. The GOR performance of Ni-P@NF obtained at different phosphorization temperatures (a) polarization curves and (b) overpotential at 50 and 100 mA cm^{-2}.

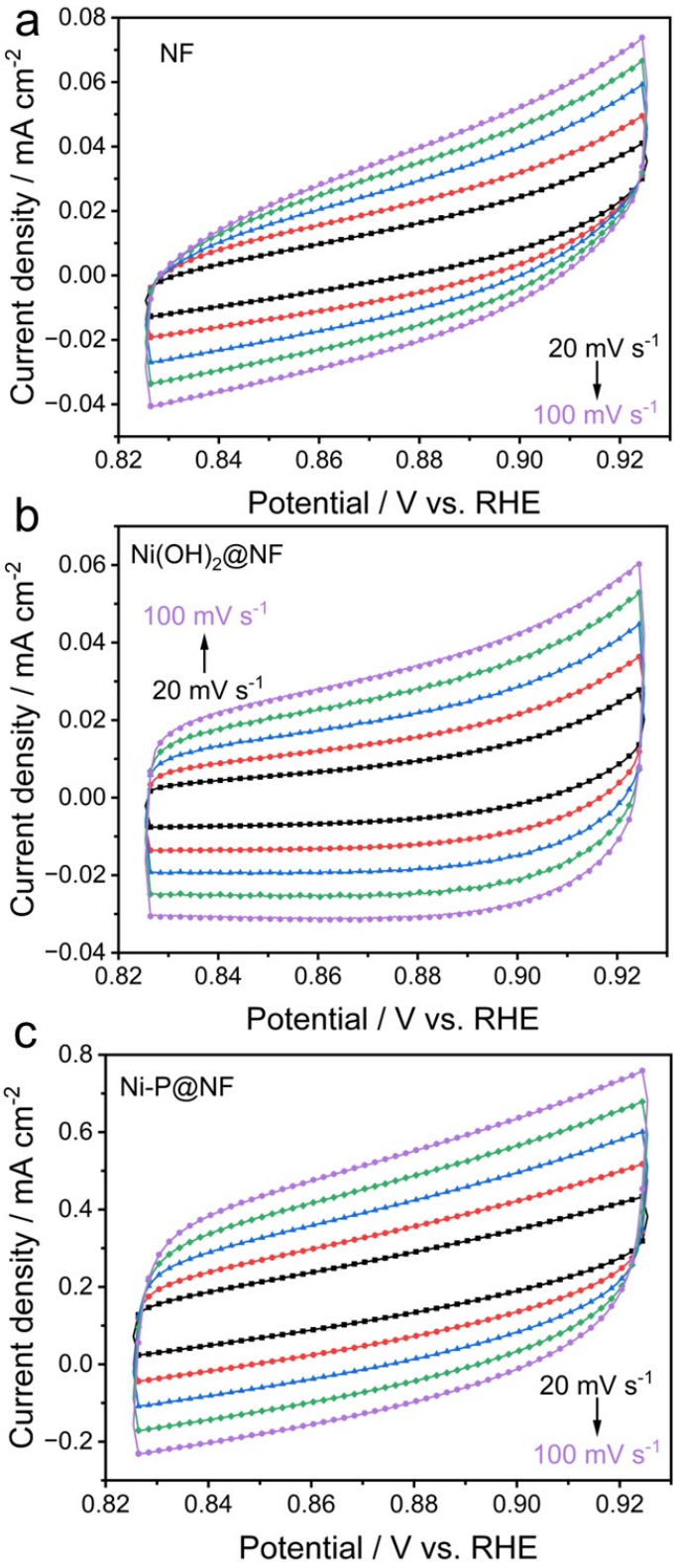

Figure S5. CV curves of (A) NF, (B) $Ni(OH)_2$@NF and (C) Ni-P@NF in the non-Faraday region at different scan rates of 20, 40, 60, 80, 100 mV s^{-1}.

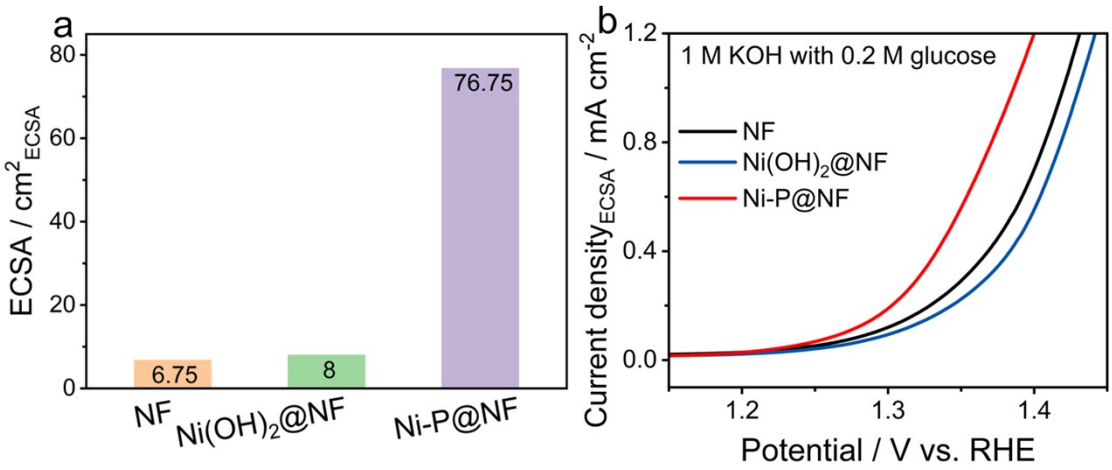

Figure S6. (a) ECSA of NF, $Ni(OH)_2$@NF and Ni-P@NF. (b) GOR performance of NF, $Ni(OH)_2$@NF and Ni-P@NF in 1 M KOH with 0.2 M glucose normalized by ECSA.

ECSA = C_{dl} /C_s (C_s = 40 μF cm^{-2})

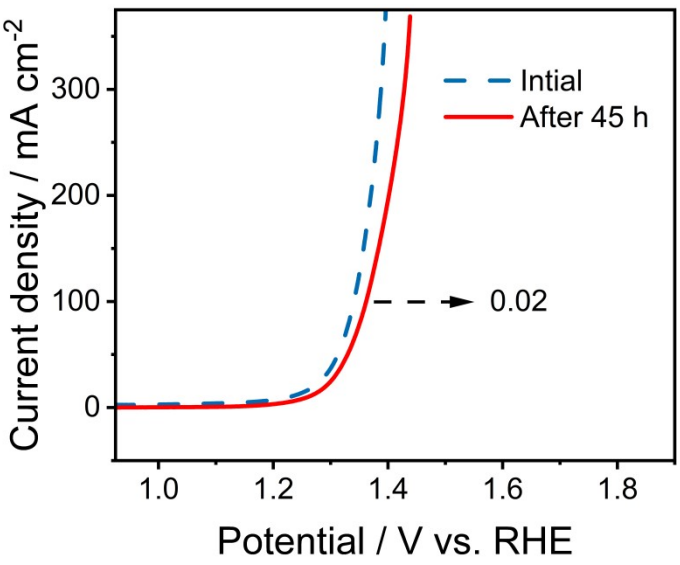

Figure S7. Comparison of the LSV curves of Ni-P@NF before and after GOR stability test in 1 M KOH with 0.2 M glucose.

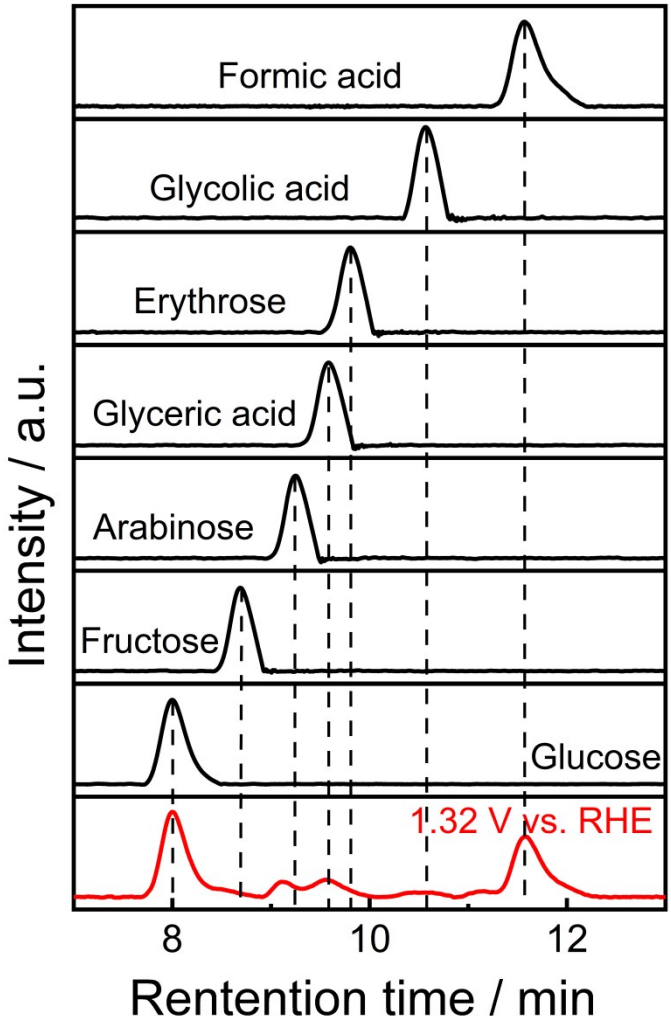

Figure S8. HPLC chromatograms of the electrolyte after GOR at 1.32 V (vs. RHE) and standard samples.

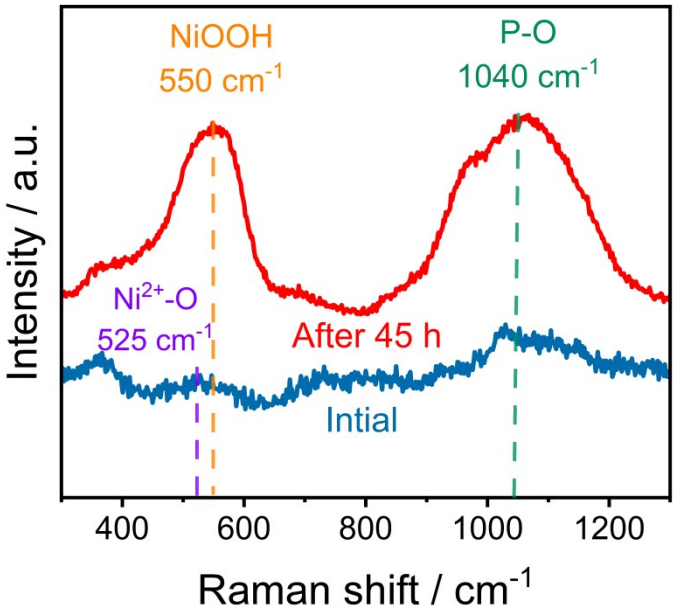

Figure S9. Raman spectra of Ni-P@NF before and after GOR testing.

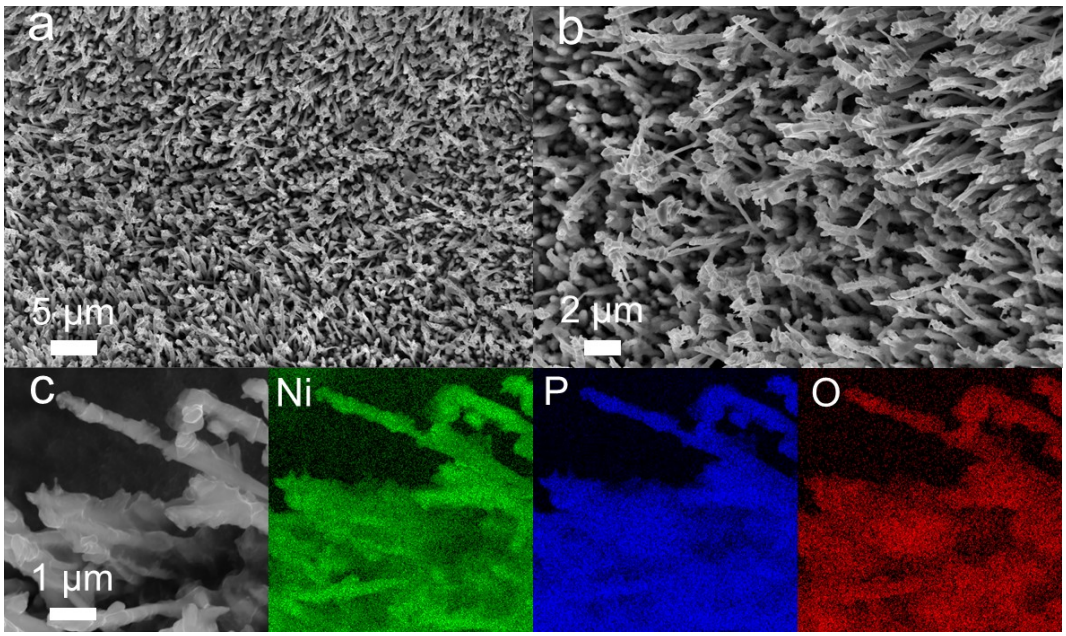

Figure S10. (a) and (b) SEM images of Ni-P@NF after GOR testing. (c) The EDS elemental mappings of Ni-P@NF after GOR testing.

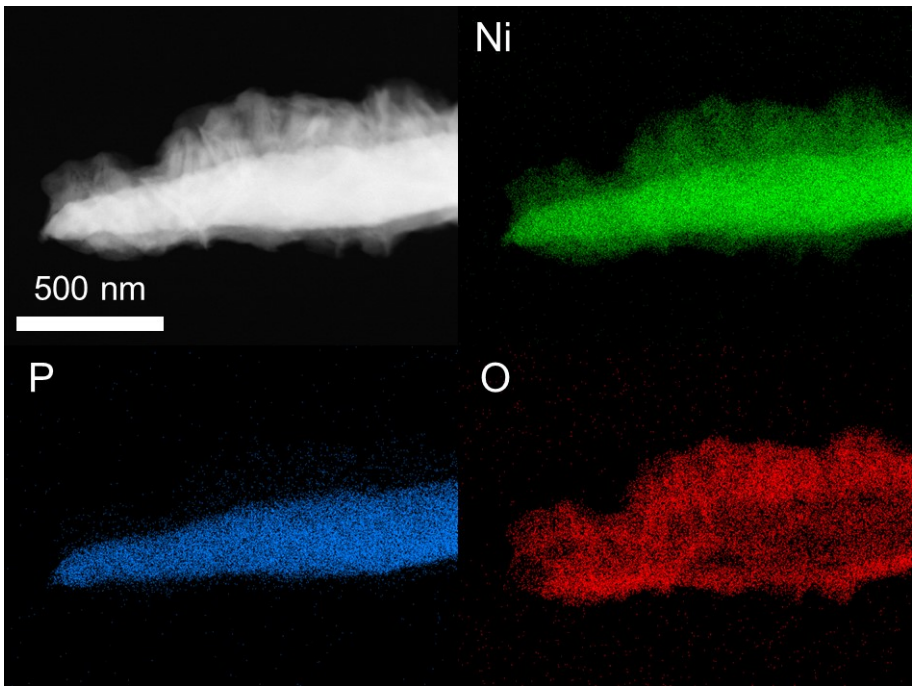

Figure S11. The EDS elemental mappings of the nanowire on the surface of Ni-P@NF after GOR testing.

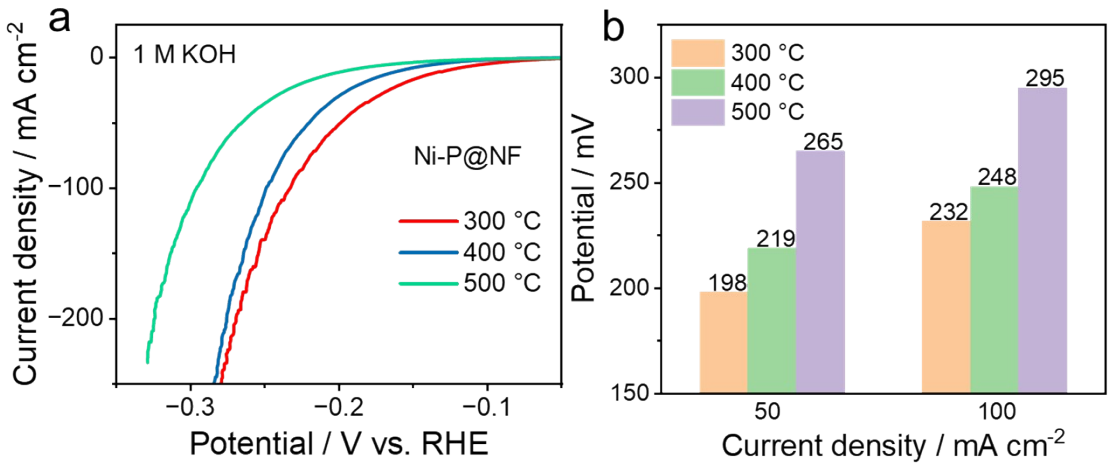

Figure S12. The HER performance of Ni-P@NF at different phosphidation temperatures of 300, 400, and 500℃. (a) Polarization curves and (b) potentials at 50 and 100 mA cm^{-2}.

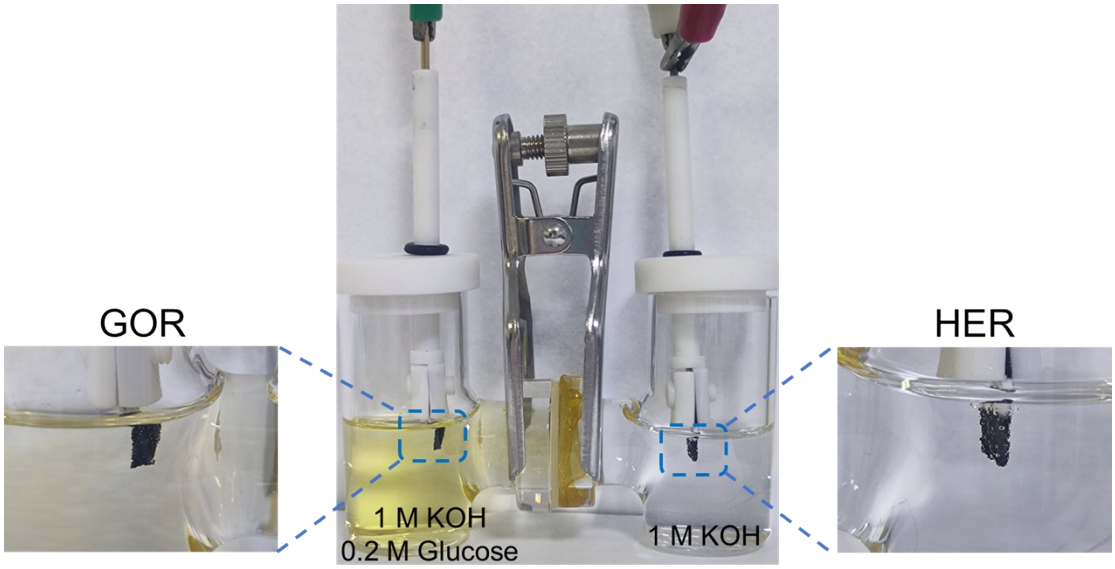

Figure S13. A digital photo of the H-type electrochemical cell.

Table S1 The comparison of GOR electrolysis activity for Ni-P@NF and other non-noble metal-based electrocatalysts.

Catalyst	Substrate	Electrolyte	Potential (V vs. RHE) @Current density (mA cm^{-2})	Ref.
Ta-NiFe LDH	0.1 M glucose	1 M KOH	1.52@50	1
$CC_{PPy}CNTs/NiCo_{300}N_2$	0.5 M glucose	1 M KOH	1.29@10	2
NiMn(1:1)On/OCNT	1 M glucose	1 M KOH	1.3@10	3
$Ni(OH)_2$-Cu_2O(S)/CF	0.01 M	1 M KOH	1.24@10	4
	5-hydroxymethylfurfural		1.39@100	
Ni_3P-Cu_3P/CF	0.01 M	1 M KOH	1.36@10	5
	5-hydroxymethylfurfural		1.44@100	
$Ni_{1.2}Cr_{0.8}P$	3 M methanol	1 M KOH	1.29@10	6
			1.43@100	
$Cu_xNi_{2-x}P$	0.01 M glycerol	1 M KOH	1.41@10	7
W-NT@NF	0.33 urea	1 M KOH	1.39@50	8
			1.43@100	
$NiMoP_x@Ni_5P_4$	1 M methanol	1 M KOH	1.36@10	9
Co@CoO-1/rGO	0.1 M glucose	1 M KOH	1.34@10	10
ReS_2/Co_9S_8	0.05 M furfural	1 M KOH	1.45@10	11
Ni-P@NF	0.2 M glucose	1 M KOH	1.22@10	This
			1.33@50	work
			1.41@100	

Table S2 EIS analyses corresponding to Nyquist curves for GOR.

	R_s (Ω)	R_{ct} (Ω)	CPE-T (F)	CPE-P (F)
NF	2.9	8.9	0.0043	0.8068
$Ni(OH)_2$@NF	2.7	7.5	0.0212	0.5441
Ni-P@NF	2.1	1.7	0.0256	0.6627

Table S3 EIS analyses corresponding to Nyquist curves for GOR-assisted water electrolysis.

	R_s (Ω)	R_{ct} (Ω)	CPE-T (F)	CPE-P (F)
NF	2.5	278.4	0.0001	0.8900
$Ni(OH)_2$@NF	2.1	51.8	0.0002	0.7835
Ni-P@NF	2.2	6.4	0.0049	0.0143

Table S4 The comparison of GOR coupled water electrolysis activity for Ni-P@NF and other non-noble metal-based electrocatalysts at 10 mA cm^{-2}.

Catalyst	Substrate	Electrolyte	Voltage (V)	Ref.
Ta-NiFe LDH	0.1 M glucose	1 M KOH	1.62	1
Ni/Ni_3N_{1-x}	0.3 M ethylene glycol	1 M KOH	1.49	12
$Ni_3PCu_3P/CF||MoNiN_x/NF$	0.01 M 5-hydroxymethylfurfural	1 M KOH	1.43	13
Co/NPC	0.1 M glucose	1 M KOH	1.56	14
$Ni(OH)_2$-$Cu_2O(S)/CF$	0.01 M 5-hydroxymethylfurfural	1 M KOH	1.44	4
$Co(OH)_2$@HOS/CP	3 M methanol	1 M KOH	1.497	15
Ni_3S_2-MoS_2/NF	0.15 M 5-hydroxymethylfurfural	1 M KOH	1.44	16
NF/PPy_{700}-Ni_3S_2-8-H_2	0.33 M urea	1 M KOH	1.5	17
$Fe_{11.1\%}$-Ni_3S_2/NF	0.33 M urea	1 M KOH	1.46	18
$ReS_2/Co_9S_8/CC$	0.05 M 5-hydroxymethylfurfural	1 M KOH	1.43	11
MoO_2-FeP@C	0.01 M 5-hydroxymethylfurfural	1 M KOH	1.486	19
$(Ni_{0.25}Fe_{0.75})_3S_2/NF$	0.33 M urea	1 M KOH	1.49	20
hp-Ni	0.01 M benzyl alcohol	1 M KOH	1.5	21
Ni_2P NPA/NF	0.01 M 5-hydroxymethylfurfural	1 M KOH	1.44	22
Ni_3S_2/NF	0.01 M 5-hydroxymethylfurfural	1 M KOH	1.58	23
Ni-P@NF	0.2 M glucose	1 M KOH	1.43	This work

References:

1. M. Tayebi, Z. Masoumi, B. Seo, C. Lim, C. H. Hong, H. J. Kim, D. Kyung and H. Kim, *ACS Appl. Mater. Interfaces*, 2024, 16, 26107-26120.
2. Y. Qiu, Y. Zhang, M. Yu, X. Li, Y. Wang, Z. Ma and S. Liu, *Small*, 2024, 20, 2310087.
3. D. Mehta, S. Kaur, N. Thakur and T. C. Nagaiah, *J. Mater. Chem. A*, 2023, 6, 11, 25507-25515.
4. G. Ren, B. Liu, X. Xu, P. Jing, J. Wu and J. Zhang, *Nano Today*, 2024, 56, 102315.
5. J. Fu, G. Yang, Y. Jiao, C. Tian, H. Yan and H. Fu, *Nano Energy*, 2024, 127, 109727.
6. U. P. Suryawanshi, U. V. Ghorpade, J. A. Yuwono, P. V. Kumar, M. A. Gaikwad, S. W. Shin, J. S. Jang, H. R. Jung, M. P. Suryawanshi and J. H. Kim, *J. Mater. Chem. A*, 2024, 12, 15127-15136.
7. L. Ma, Y. Miao, J. Yang, Y. Fu, Y. Yan, Z. Zhang, Z. Li and M. Shao, *Adv. Energy Mater.*, 2024, 14, 2401061.
8. M. Liu, W. Zou, S. Qiu, N. Su, J. Cong and L. Hou, *Adv. Funct. Mater.*, 2023, 34, 2310155.
9. B. Zhu, J. Xiong, S. Wu, K. You, B. Sun, Y. Liu, M. Chen, P. Jin and L. Feng, *Adv. Funct. Mater.*, 2024, 34, 2407236.
10. M. Wu, J. Zhao, C. Li and R. Liu, *J. Mater. Chem. A*, 2022, 10, 4791-4799.
11. Q. Pang, K. Sun, X. Fan, K. Xiang, B. Li, S. Zhao, Y. D. Kim, Q. Liu, Z. Liu and Z. Peng, *Chem. Eng. J.*,2024, 497, 154475.
12. C. Zhou, C. Jia, X. Xiang, L. Wang, S. Wu, N. Zhang, S. Zhao, G. Yang and Y. Chen, J. Mater. Chem. A, 2024, 12, 15772-15780.
13. J. Fu, G. Yang, Y. Jiao, C. Tian, H. Yan and H. Fu, *Nano Energy*, 2024, 127, 109727.
14. D. Li, Y. Huang, Z. Li, L. Zhong, C. Liu and X. Peng, *Chem. Eng. J.*, 2022, 430, 132783.
15. K. Xiang, D. Wu, X. Deng, M. Li, S. Chen, P. Hao, X. Guo, J. Luo and X. Fu, *Adv. Funct. Mater.*, 2020, 30, 1909610.

16. S. Yang, Y. Guo, Y. Zhao, L. Zhang, H. Shen, J. Wang, J. Li, C. Wu, W. Wang, Y. Cao, S. Zhuo, Q. Zhang and H. Zhang, *Small*, 2022, 18, 2201306.
17. Y. Zhang, Y. Qiu, Y. Wang, B. Li, Y. Zhang, Z. Ma and S. Liu, *ACS Appl. Mater. Interfaces*, 2021, 13, 3937-3948.
18. W. Zhu, Z. Yue, W. Zhang, N. Hu, Z. Luo, M. Ren, Z. Xu, Z. Wei, Y. Suo and J. Wang, *J. Mater. Chem. A*, 2018, 6, 4346-4353.
19. G. Yang, Y. Jiao, H. Yan, Y. Xie, A. Wu, X. Dong, D. Guo, C. Tian and H. Fu, *Adv. Mater.*, 2020, 32, 2000455.
20. C. Liu, F. Li, S. Xue, H. Lin, Y. Sun, J. Cao and S. Chen, *ACS Appl. Energy Mater.*, 2022, 5, 1183-1192.
21. B. You, X. Liu, X. Liu and Y. Sun, *ACS Catal.*, 2017, 7, 4564-4570.
22. B. You, N. Jiang, X. Liu and Y. Sun, *Angew. Chem. Int. Ed.*, 2016, 9913.
23. B. You, X. Liu, N. Jiang and Y. Sun, *J. Am. Chem. Soc.*, 2016, 138, 41, 13639-13646.